Liquid Metal Embrittlement of Silver by Lead

Annealed silver is made highly susceptible to embrittlement with stress-assisted grain boundary penetration of lead

BY J. A. WASYNCZUK, G. W. HENDERSON AND F. D. ROSS

ABSTRACT. The susceptibility of annealed Ag to embrittlement by liquid Pb was evaluated with small cantilever beams that were subjected to dead loads at 338°C. When the resulting tensile stress was more than 40% above the proportional limit, rapid intergranular fracture was nearly coincident with the application of load. For bending stresses close to the proportional limit, delayed failure was observed. Stress-assisted grain boundary penetration of Pb was evident in all cases.

Introduction

Liquid metal embrittlement (LME), defined as the reduction in ductility that can occur when normally ductile metals or alloys are stressed while in contact with liquid metals, has been the subject of several reviews (Refs. 1–8). Solid-substrate/liquid-metal combinations that exhibit LME are termed embrittlement couples (Refs. 1–8). Embrittlement is usually most severe at temperatures slightly above melting, and at higher temperatures a brittle-to-ductile transition is often observed (Refs. 1–8). With the application of a sufficiently high tensile stress, failure by LME can be extremely rapid. Situations in which the simultaneous application of stress and liquid metal result in nearly instantaneous failure have been categorized as adsorbtion-induced (Refs. 3, 5, 7) or classic (Ref. 6) LME. Although in some cases of adsorbtion-induced LME the liquid metal can penetrate substrate grain boundaries, data indicate that it is not a requirement for catastrophic failure (Refs. 1–8). Liquid metal embrittlement can also be manifested as delayed failure (Refs. 1–11), and in some cases grain boundary penetration appears to be central to the fracture mechanism (Refs. 10, 11). Although strong solid-liquid bonding (Ref. 12) and constitutional characteristics, such as limited mutual solubility and the absence of intermediate phases (Refs. 1–7), or the occurrence of a eutectic with a small but definite solubility of the embrittling liquid in the solid are common to many embrittlement couples (Refs. 2, 12), exceptions defy a universally applicable rule for predicting susceptibility to LME. Because the severity of embrittlement can be very sensitive to temperature range, strain rate and microstructure (Refs. 1–8), the number of reported LME couples is likely to expand as wider variations in use and test conditions are encountered (Ref. 7).

It has been reported that Ag is embrittled by liquid Hg, Ga and Li (Refs. 1–8, 13–15), with embrittlement by Ga being more severe than by Hg (Refs. 13–15). The embrittling tendencies of both these liquid metals are modified by additions of In (Ref. 14). Silver-gold alloys and Ag-2wt-%Cu are also embrittled by Hg and Ga (Refs. 15, 16). At room temperature, LME of statically loaded Ag by both Hg and Ga is characterized by a well-defined critical stress, above which failure occurs in < 1 s, but below which failure does not occur in >2000 s (Ref. 14). Since exposing the Ag to Ga for as much as 2 h prior to loading did not change this critical stress, it was concluded that intergranular penetration was not a factor in this adsorbtion-induced form of LME (Ref. 14). For Ag with a 125-μm grain size, the Ag/Ga embrittlement couple displayed a brittle-to-ductile transition at approximately 60°C (Ref. 13).

Silver-based alloys are widely used as electrical contact materials, and Pb-rich alloys are common high-temperature solders. Silver and Pb form a simple eutectic at 304°C, 95.5 at.-%Pb (Ref. 17). The solubility of Ag in Pb is very low (Ref. 18), and a tie-line at the melting temperature of Pb (327.5°C) intersects the Ag liquidus and solidus at approximately 96.1 and 2.4 wt-%Pb, respectively (Ref. 17). Although joints are typically designed such that the members being soldered are relatively free of stress, it is not extraordinary for solder to flow onto regions under residual stresses, such as those resulting from lead forming. However, reports on the embrittlement of Ag or its alloys by Pb or its alloys were not uncovered by extensive literature searches. The present work was performed to characterize this unreported embrittlement couple.

KEY WORDS

Ag-Based Alloys
Pb-Rich Alloys
Soldering
Bending Stress
LME
Embrittlement

Experimental

The susceptibility of Ag to LME by Pb was evaluated with small dead-loaded cantilever beams. The cross section of these beams measured 0.35 X 1.59 mm, and the distance from the clamped end to the loading pin was 6.35 mm. The beams were made from platelets of 99.9% Ag that were cold rolled from 1.65 to 0.38 mm thick, then annealed for 1 h at 450°C in air. This anneal produced a fully recrystallized microstructure with an average grain size of 18 μm. This grain size is the mean linear intercept diameter, defined as the test line length divided by the number of intersections with boundaries. Intersections with twin

J. A. WASYNCZUK, G. W. HENDERSON and F. D. ROSS are with The Aerospace Corp., Los Angeles, Calif.

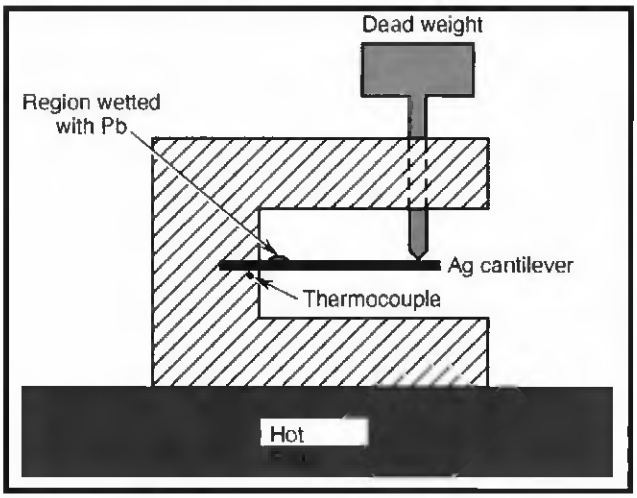

Fig. 1 — Schematic of the testing apparatus.

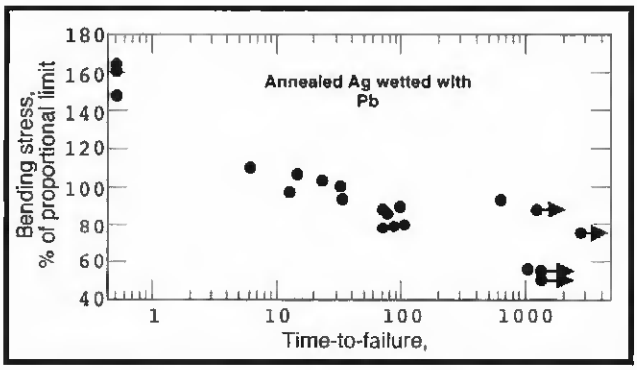

Fig. 2 — The observed relationship between applied stress and time to failure. Arrows indicate specimens that did not fail.

boundaries were included in these measurements. The microhardness of this recrystallized Ag was found to be 52 HK (100-g load).

After being sawed from the annealed strip, the broad faces of the beams were lapped to the appropriate thickness with 600-grit SiC paper. A small area of what would become the surface under tension was then wetted with Pb. By briefly placing a beam on a hot plate that was maintained at 338 ±2°C, an approximately 0.1 mg sliver of 99.999% Pb was melted on a broad face, close to what would become the clamped end of the cantilever. Wetting was promoted by a paste flux that contained zinc chloride and ammonium chloride (NOKORODE, The M. W. Dunton Co., West Warwick, R.I.). It was found that the flow of the liquid Pb was enhanced parallel to the lapping direction, which was always normal to the length of the beam. Following this wetting operation, the samples were thoroughly cleaned in isopropyl alcohol. Subsequent testing was performed in air, without flux. A schematic of the testing apparatus is shown in Fig. 1.

After a beam was clamped into the fixture, it was placed on a hot plate that was controlled such that the temperature at the clamp would stabilize at 338 ± 2°C. The load was applied immediately after this temperature was reached, within 3 min of placing the fixture on the hot plate. Given the proximity of the wetted region to the 6061 aluminum fixture, and the high thermal conductivities of Ag and 6061 Al, the temperature measured with the thermocouple is estimated to be no more than a few degrees higher than the sample at its fracture location. Testing was terminated either upon the observation of fracture or after the specimen had experienced at least 20 min at 328°C. Upon completion of the test, the fixture was transferred to a large aluminum chill block.

The short-term bending strength was determined with an Instron load frame, configured such that the crosshead lifted a clamped beam up to a quartz rod that was connected to a load cell. An oven that surrounded the fixture maintained the temperature at 338 +7/-0°C. The crosshead displacement rate was 0.02 mm s^{-1}. A standard elastic beam-bending formula was used to calculate the maximum bending stress at the clamped end of the cantilever (Ref. 19). The reported values represent the average of at least four tests.

Metallographic cross sections were prepared by standard mechanical grinding and polishing methods. Of the several etchants that were tried, a solution prepared from 10 g ammonium persulfate, 10 g potassium cyanide and 400 ml deionized water proved to be most useful. It revealed the grain structure of the Ag and only mildly attacked the Pb-rich phase. To facilitate scanning electron microscopy (SEM), 36% HCl was sometimes used to dissolve Pb from the Ag fracture surfaces. SEM and windowless energy-dispersive X-ray spectroscopy (EDS) were performed with a JEOL 840 instrument, operated at 15 or 20 kV.

Results

Using the standard elastic beam-bending formula, proportional limits at room temperature and 338°C were found to be 167 ± 26 MPa and 80 ± 3 MPa, respectively. The observed relationship between the applied stress, reported as a percentage of the proportional limit at 338°C, and the time to failure is illustrated in Fig. 2. Load is reported as a percentage of the proportional limit at 338°C. When the resulting tensile stress exceeded the proportional limit by more than 40%, fast fracture was nearly coincident with the application of load. In Fig. 2, this behavior is represented by a 0.5-s time to failure. At the low end of the investigated stress range, most of the specimens loaded to ≤ 75% of the proportional limit did not fail within the ≥ 20-min time limit of the experiment. At intermediate loads, the time to failure was highly variable. In all cases of delayed failure, however, brittle fracture occurred suddenly and rapidly. Although the application of loads that resulted in stresses near the proportional limit caused an immediate deflection that was readily noticed, subsequent subcritical deflections were imperceptible by the unaided eye.

As exemplified in the backscatter SEM image shown in Fig. 3, liquid Pb-assisted fracture typically occurred toward the boundary of the wetted region, within 0.5 mm from the clamped end of the beam. Figure 3 also reveals infiltration of the fracture with Pb-rich material, which appears light due to the higher atomic number of Pb. Following dissolution of the Pb-rich material that coated much of the fracture surface, it became apparent that liquid Pb-assisted fracture of Ag was intergranular, as exemplified by the secondary electron image shown in Fig. 4. In some cases, particularly with the specimens that exhibited short failure times, meaningful fractography was accomplished without dissolving the Pb-rich coating. A backscatter electron image of such an as-fractured surface is shown in Fig. 5. This image highlights the intergranular fracture mode and also reveals Pb-rich intergranular films, which appear as regions of light contrast. SEM fractography also revealed that intergranular secondary cracking was common in these liquid Pb-assisted fractures. In addition to revealing the fracture mode, SEM observations of rounded grain edges, such as shown in Fig. 4, Ag-rich particles within the Pb-rich phase, and modification of the topography of the lapped Ag surfaces indicated that wetting was accompanied by dissolution of the Ag.

The results of SEM examination of cross-sectioned specimens reinforced the fractographic evidence of intergranular fracture and grain boundary penetration. These characteristics were most clearly observed in etched cross sections. A backscatter electron image of a cross section that displayed pronounced intergranular secondary cracking is shown in Fig. 6. For this specimen, crack opening was intentionally restricted by placing a stop beneath the loaded end of the beam. The results of close SEM examination of both etched and as-polished cross sections indicated that the mottled appearance of the Pb-rich material is largely due to Ag-rich particles, which were attacked by the etchant. Most of these Ag-rich particles could be categorized as either large (microns in diameter) and equiaxed, or small (submicron diameter) and rod-shaped. Following dissolution of the Pb in HCl, nests of the rod-shaped particles remained attached to the Ag fracture surface and the wetted broad face of the specimen. When such nests of particles were examined by windowless EDS, only Ag was detected. This composition, and the rod morphology, are consistent with the Ag-rich eutectic microconstituient (Ref. 20). The large equiaxed particles appeared to be grains that separated from the substrate and floated in the Pb.

SEM examination of cross sections also revealed Pb-rich intergranular films in the uncracked portions of failed specimens, as well as in the specimens that did not fail. Although these Pb-rich films could be imaged in the as-polished condition, resolution was improved by etching. A backscatter electron image of a typical Pb-rich intergranular film is shown in Fig. 7A. Although the etchant was particularly aggressive on the Ag grain boundaries, discontinuous films of Pb-rich material were preserved. The X-ray maps shown in Fig. 7B and C confirm that the light contrast of the intergranular films in the backscatter image is largely due to atomic number contrast. These Pb-rich intergranular films also appeared discontinuous in as-polished cross sections. In cross sections of the specimens that did not fail under load, these intergranular Pb-rich films were observed as far as 200 μm from the wetted surface under tension, or roughly halfway through the specimen thickness. In contrast to these loaded specimens, no Pb-rich intergranular films were found in cross sections of unloaded specimens that experienced up to 15 min at 338°C.

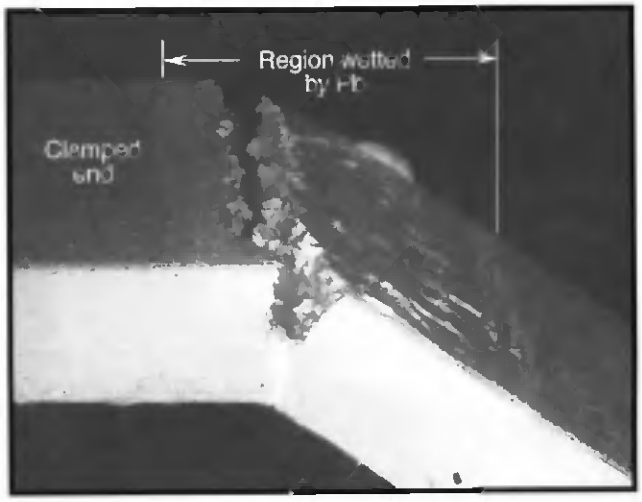

Fig. 3 — Backscatter electron image of a fractured beam.

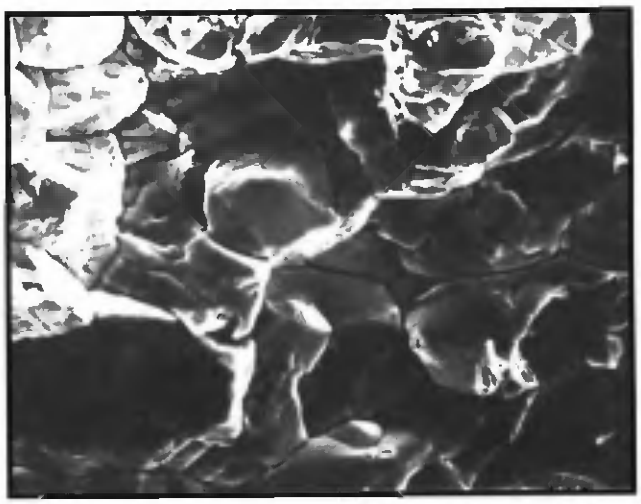

Fig. 4 — Secondary electron image of a fracture surface, after the Pb-rich coating was removed by exposure to HCl.

Fig. 5 — Backscatter electron image of an as-fractured surface.

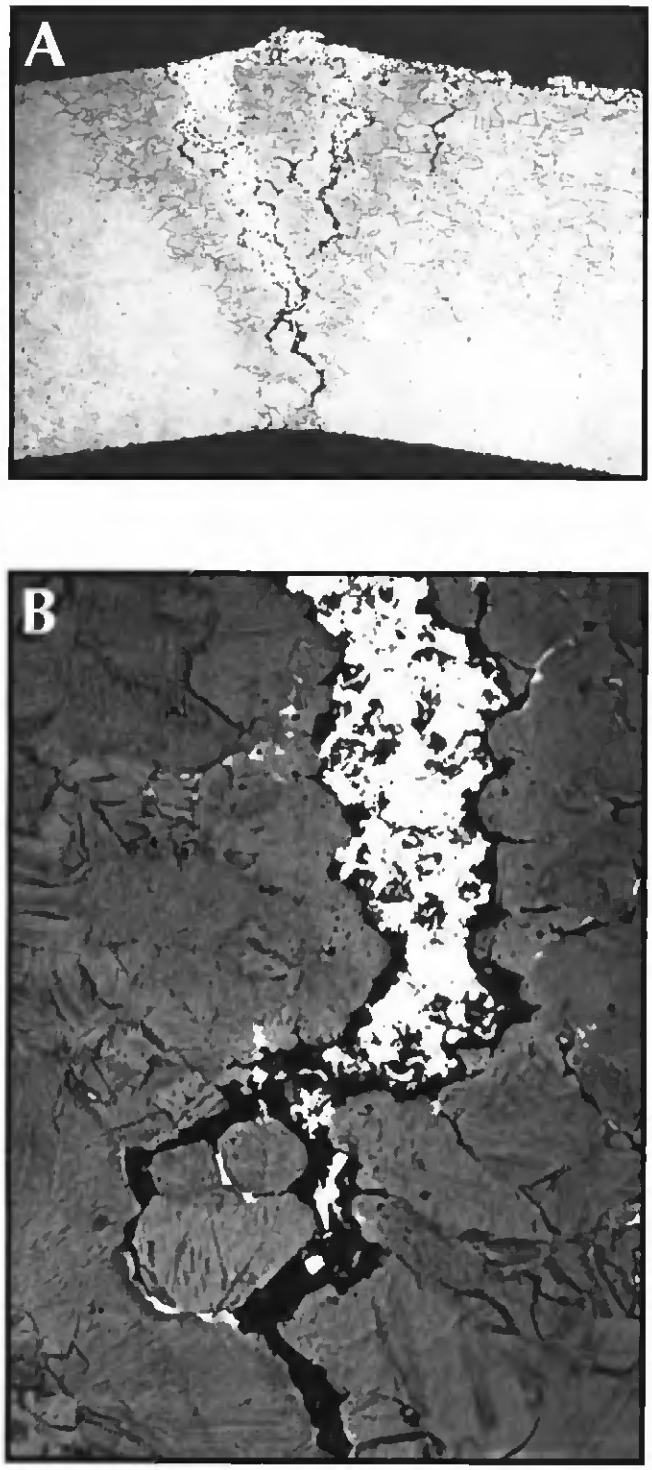

Fig. 6 — Backscatter electron images of a polished and etched cross section. The clamped end of the cantilever is to the left. A magnified view of the Pb-infiltrated crack is shown in B.

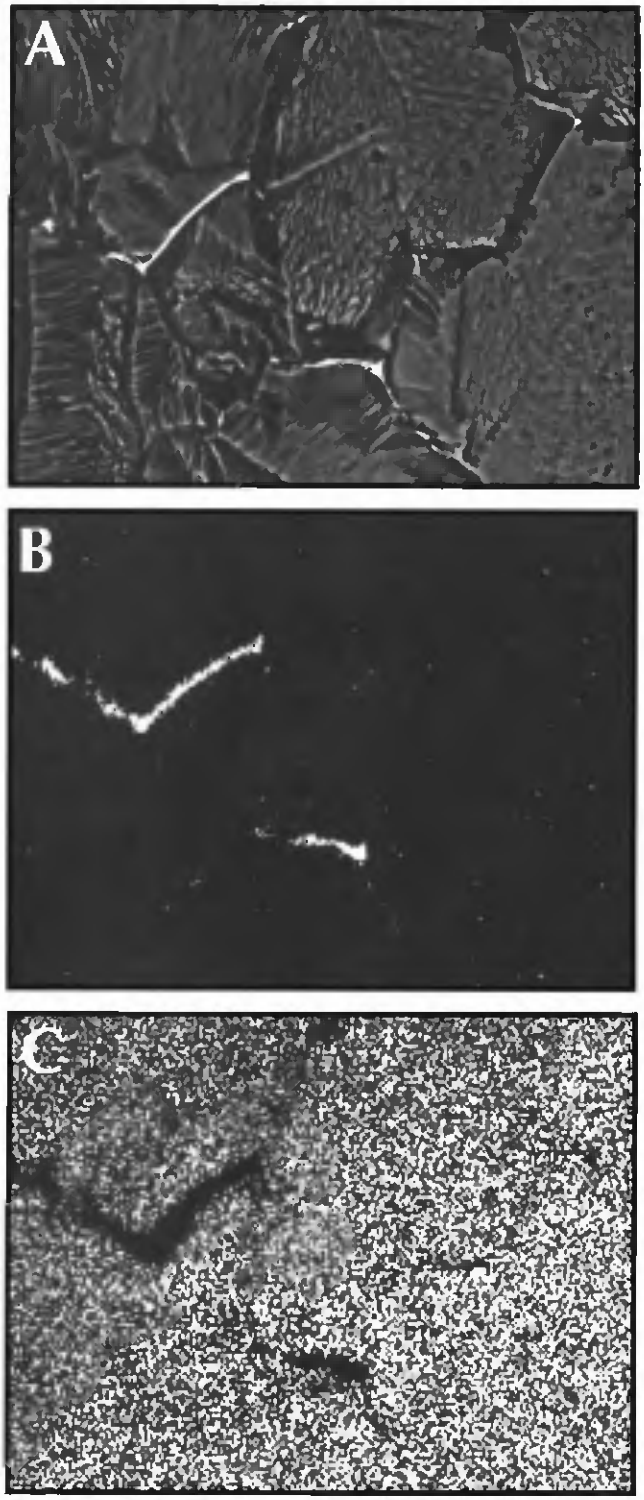

Fig. 7 — A — Backscatter electron image of a polished and etched cross section; B, C — X-ray maps of Pb and Ag, respectively.

Discussion

The finding that liquid Pb promotes intergranular fracture of Ag is consistent with the general trend for LME of polycrystalline fcc metals to be intergranular (Refs. 1–8, 10, 11, 13–16). The finding that brittle intergranular fracture was nearly coincident with the application of loads sufficient to induce plastic deformation is also consistent with the attributes of adsorbtion-induced (Refs. 1–8) or classic (Ref. 6) LME. However, the substrate dissolution, stress-assisted grain boundary penetration and delayed failure behavior observed in the present work are distinct from the adsorbtion-induced behavior reported for couples such as Ag-Ga and Ag-Hg (Refs. 13–15). It is likely that the relatively high substrate homologous temperature employed, roughly 50%, contributed to the extent of these solid-liquid reactions and the delayed failure behavior (Ref. 1).

As has been done to investigate LME of Al by Zn (Ref. 21), lower substrate homologous temperatures can be achieved by alloying the embrittler. Data generated in our laboratory indicate that Bi, which melts at 271.4°C, can also induce catastrophic LME of annealed Ag. Bismuth forms a simple eutectic with Ag (262.5°C, 0.7 at.-% Bi [Ref. 17]), and is a major component in many low-temperature solder alloys. Experiments with the PbBi eutectic (125.5°C, 45 at.-% Bi [Ref. 17]) might further expand the range over which Ag is susceptible to LME.

Although the present results indicate that stress-assisted grain boundary penetration is important in the delayed cracking behavior exhibited by the Ag/Pb embrittlement couple, additional work will be required to elucidate the failure mechanism. Since metallographic evidence of penetration was found as deep as the midthickness of specimens that did not fail at loads as high as 88% of the proportional limit, and the bending strength of a cantilever scales inversely with the square of its thickness (Ref. 19), it is clear that the observed penetration could not have caused more than a slight reduction in the strength of the polycrystalline silver. This retention of strength is similar to the behavior reported for LME of a Cu-2wt-%Be alloy by a Hg-2wt-%Na amalgam, an embrittlement couple in which grain boundary penetration was shown to be a precursor to delayed failure (Ref. 10).

The occurrence of a eutectic with a small but definite solubility of the embrittling liquid in the solid (Refs. 5, 12) is a subset of the general, but not universal, trend that the phase diagrams of embrittlement couples usually display limited mutual solubility and an absence of intermediate phases (Refs. 1–8). Since wetting of most commercial solder alloys is accompanied by intermetallic formation, it may appear that the practical consequences of the present work are few. However, our first encounter with LME of Ag by Pb involved a Ag-rich electrical contact alloy that was joined by a Pb-1.5Ag-1Sn solder, which melts at approximately 318°C. Experiments with annealed Ag revealed that the kinetics of intermetallic formation on the substrate are sluggish with this solder, and that the characteristics of LME induced by this Pb-1.5Ag-1Sn alloy are similar to those observed with pure Pb.

Conclusion

The results of simple beam-bending experiments indicate that annealed Ag is susceptible to LME by Pb at 338°C. When the resulting tensile stress was 40% higher than the proportional limit, this embrittlement couple displayed rapid intergranular fracture that was nearly coincident with the application of load. Delayed failure was observed at stresses near the proportional limit. Stress-assisted grain boundary penetration was observed in all cases.

Acknowledgments

The metallographic specimens were prepared by J. Marcus and J. C. Uht assisted with SEM/EDS. The authors also appreciate helpful discussions with R. DePace, TRW Space & Electronics Group.

References

1. Rostoker, W., Markus, H., and McCaughey, J. M. 1960. *Embrittlement by Liquid Metals*, Reinhold Publishing Co., New York, N.Y.

2. Stoloff, N. S. 1967. *Surfaces and Interfaces II, Physical and Mechanical Properties*. J. J. Burke, N. L. Reed and V. Weiss, eds., Syracuse University Press, pp. 157–182.

3. Westwood, A. R. C., and Latanision, R. M. 1969. *Corrosion by Liquid Metals*. J. E. Draley and J. R. Weeks, eds., Plenum Press, New York, N.Y., pp. 441–447.

4. Shunk, F. A., and Warke, W. R. 1974. *Scripta Met.*, Vol. 8, pp. 519–526.

5. Stoloff, N. S. 1979. *Environment-Sensitive Fracture of Engineering Materials*. Z. A. Foroulis, ed., Metallurgical Society of AIME, Warrendale, Pa., pp. 486–518.

6. Nicholas, M. G., and Old, C. F. 1979. *J. Mat. Sci*, Vol. 14, pp. 1–18.

7. Stoloff, N. S. 1984. *Embrittlement by Liquid and Solid Metals*. M. H. Kamdar, ed., The Metallurgical Society of AIME, Warrendale, Pa., pp. 3–26.

8. Nicholas, M. G., *ibid*, pp. 27–50.

9. Gordon, P., and An, H. H. 1982. *Met. Trans. A*, Vol. 13A, pp. 457–472.

10. Rinnovatore, J. V., Corrie, J. D., and Markus, H. 1966. *Trans. ASM*, Vol. 59, pp. 665–671.

11. Ichinose, H., and Takashima, T. 1984. *Embrittlement by Liquid and Solid Metals*. M. H. Kamdar, ed., The Metallurgical Society of AIME, Warrendale, Pa., 1984, pp. 197–209.

12. Kelley, M. J., and Stoloff, N. S. 1975. *Met. Trans. A*, Vol. 6A, pp. 159–166.

13. Preece, C. M., and Westwood, A. R. C. 1969. *Trans. ASM*, Vol. 62, pp. 418–425.

14. Preece, C. M., and Westwood, A. R. C. 1969. *Fracture 1969: Proc. of the Second Intl. Conf. on Fracture*. P. L. Pratt, ed. Chapman and Hall, London, pp. 439–449.

15. Preece, C. M., and Westwood, A. R. C. 1969. *Corrosion by Liquid Metals*. J. E. Draley and J. R. Weeks, eds., Plenum Press, New York, N.Y., pp. 441–447.

16. Stoloff, N. S., and Seelinger, S. 1973. *Proc. Conf. In-Situ Composites II, Mechanical Properties*. NMAB 308-II, National Research Council, Washington, D.C., pp. 223–236.

17. *Binary Alloy Phase Diagrams*. 1990. Second Edition, Vol. 1, T. B. Massalski ed., ASM International, Materials Park, Ohio.

18. Campbell, A. N., Tsao, S. S., and Turnbull, D. 1987. *Acta metall.*, Vol. 35, pp. 2453–2464.

19. Popov, E. P. 1976. *Mechanics of Materials*, Second Edition, Prentice-Hall, Englewood Cliffs, N.J., p. 580.

20. Collins, G. G., Smith, I. O., and Chadwick, G. A. 1978. *Matl. Sci. and Eng.*, Vol. 36, pp. 1–9.

21. Mae, T., and Hori, S. 1991. *J. Matl. Sci.*, Vol. 26, pp. 479–483.